Radar RFI at Goldstone DSS 12 and DSS 16

S. D. Slobin and T. K. Peng
Telecommunications Systems Section

Radio frequency interference (RFI) from the DSS 14 Goldstone Solar System Radar (GSSR) was investigated at DSS 12 and DSS 16 with the goal of assisting in the choice of the location of future DSN antennas. Total power measurements at both locations were made at the S-band carrier frequency of 2320 MHz. X-band measurements at the carrier frequency of 8495 MHz could not be made. Exciter-chain output spectrum and klystron output spectrum measurements were made at S- and X-bands using a probable worst-case modulation of the radar signal (short pseudorandom number [PN] code length and short pulse length). Based on these measurements it is estimated that RFI levels in the DSN receiving bands at both sites (above 10-deg elevation) would be below −192 dBm for a 1-Hz bandwidth.

I. Introduction

During January through May 1989, a series of tests was carried out at Goldstone to determine whether S- and X-band solar system radar experiments using the DSS 14 70-m antenna would create radio frequency interference (RFI) at new DSN receiving antennas which might be located at the present DSS 12 or DSS 16 sites. All tests were carried out in clear weather. The S-band radar frequency is 2320 MHz, and the DSN downlink band extends from 2200 to 2300 MHz. The X-band radar frequency is 8495 MHz, and the DSN downlink band extends from 8400 to 8440 MHz.

Modulating the radar signal causes power to extend away from the carrier frequencies; depending on the pulse and code lengths of the modulation, this power may be a problem to spacecraft signal reception. The power level decreases with frequency away from the carrier; therefore received power is highest at the upper end of the S- and X-receiving bands. DSS 16 does not have an X-band receiver and the DSS 12 X-band receiver would not tune up as high as 8495 MHz. The modulated radar signals were estimated to be too weak to be received by the DSN receivers, yet the RFI requirements were below even that low level of detectability.

A primary driver for the RFI measurements was the need to determine a low-noise location for the new 34-m beam-waveguide DSN receiving antenna at Goldstone (DSS 18). Colocation with the existing 26-m antenna (DSS 16) was under consideration.

The plan for doing these tests was as follows:

(1) Make received-power measurements at the S- and X-band radar carrier frequencies at DSS 12 and DSS 16. These measurements would be made using all orientations of the transmitting and receiving antennas. X-band measurements were later found impossible to make with existing equipment.

(2) Using the *total* received power levels, predict the worst-case received power per spectral line at the tops of the DSN receiving bands under the condition of worst-case modulation (short pulse length and short code length). Included in this modeling is an estimate of the radar-transmitter input and output filtering.

(3) Measure the transmitter exciter-chain output spectrum (klystron-amplifier input spectrum) and klystron output spectrum at DSS 14 to verify estimates used in the RFI modeling.

(4) Determine whether deduced power at the top of the receiving bands exceeds the DSN limit of −192 dBm per 1-Hz bandwidth. This limit is 6 dB below the noise power of a 20-K system (6 dB below −186 dBm).

The following tests were carried out:

(1) January 27, 1989: S-band total-power RFI at DSS 16 (26-m, X-Y antenna)

(2) February 27, 1989: S-band total-power RFI at DSS 12 (34-m, HA-Dec antenna)

(3) March 31, 1989: S-band total-power RFI at DSS 12

(4) April 9, 1989: S- and X-band radar modulation spectrum at klystron input (exciter-chain output) at DSS 14

(5) May 17, 1989: S-band total-power RFI at DSS 16

(6) May 22, 1989: S- and X-band radar modulation spectrum at klystron output at DSS 14

Throughout the test period, there were FAA and USAF restrictions placed on both transmitter power and transmitter pointing. At high power (400 kW, S-band), the DSS 14 antenna could not point lower than 15-deg elevation; below that, down to 10.6 deg, the power was limited to 105 kW. The X-band restrictions, had that frequency been used, would have been more severe due to the much higher X-band gain of the transmitting antenna. In addition, azimuth restrictions were placed on DSS 14 pointing. Sometimes the DSS 14 antenna could point toward the receiving antenna; sometimes that azimuth was totally off-limits. During one test (Test 5), there was one azimuth restriction for the first half and another during the second half, and only then was it possible to point directly toward DSS 16. The two sets of received-power data thus represented two different multipath/refraction conditions, and it was necessary to merge these data in an indirect way in order to create a consistent set of full-sky data at the receiving antenna. Considering the azimuth, elevation, and power restrictions of the transmitting antenna, and the pointing differences and restrictions of the receiving antennas (DSS 16 is mechanically restricted from looking at the horizon due east or west; DSS 12 cannot look near the northern horizon toward DSS 14), only with great difficulty were the disparate data sets merged to create a consistent RFI model of the Goldstone environment.

II. RFI Field Test Results

A. Test 1 (DSS 16, S-Band, Total Power, January 27, 1989)

Figure 1 shows a received radar continuous wave (CW) signal as seen on a spectrum analyzer display during the first DSS 16 test. The view here is a 100-kHz portion of the IF band, centered at 520 MHz. Adjacent to the radar signal is a calibrated test signal, which is injected in front of the station's low-noise amplifier (S-band paramp). In this case, the test signal is offset 10 kHz below the radar signal and has an amplitude of −70 dBm. Thus, the received radar signal is determined to have a strength of −83 dBm. These are CW (single-line) signals and thus are of "infinitesimal" width. The line widths shown in the figure are convolutions of the individual lines and the 100-Hz resolution bandwidth of the spectrum analyzer. It should be noted that this was the highest-strength signal received during any of the tests and arose because both the DSS 14 antenna (transmitting 100 kW) and the DSS 16 receiving antenna were pointed at low elevation angles toward a group of hills located west of Goldstone Lake. These relative antenna orientations would not be used during normal radar and spacecraft tracking operations. The noise floor of the spectrum analyzer is shown to be −130 dBm (for the 100-Hz resolution bandwidth). With the narrowest resolution bandwidth available (10 Hz), radar signals as low as −140 dBm would be visible.

Figure 2 shows a series of received power measurements made at 2320 MHz on the DSS 16 antenna pointing at an elevation angle of about 4.5 deg, as low as the antenna could point along the horizon. At the DSS 16 azimuth of about 292 deg ($Y = -68$ deg), there exist a number of hills west of Goldstone Lake rising to a height of 1000 to 1500 ft above the elevation of DSS 16. With both antennas pointing toward those hills, received powers in the −83-dBm to −90-dBm range were observed (depending on the elevation angle of DSS 14). This type of isolated high RFI is referred to as a "hot spot." With DSS 14 pointing toward DSS 16, and DSS 16 pointing toward DSS 14 (azimuth = 351.4 deg, $Y = -8.6$ deg), powers in the range of −105 dBm to −120 dBm were observed,

with DSS 14 transmitting both 400 kW and 100 kW at low elevation angles. At other azimuths along the northern horizon (4.5-deg elevation), DSS 16 received powers as low as −127 dBm.

Based on far-field assumptions of antenna gain as a function of angle off beam peak, it was predicted that for the case of the two antennas pointing at each other (DSS 14, 400 kW, 15-deg elevation, and DSS 16, 4.5-deg elevation, 9.7 km apart), the received power at DSS 16 would be −14 dBm, from which one would infer a terrain/hill isolation effect of at least 91 dB. Even if the DSS 14 off-axis gain is 30 dB lower than modeled (due to incorrect far-field assumptions), the inferred hill isolation would still be 61 dB, a probable lower limit to the effect of the terrain.

B. Test 2 (DSS 12, S-Band, Total Power, February 27, 1989)

Figure 3 shows received power levels at the DSS 12 HA-Dec antenna. For the limited set of measurements, received powers lie in the −120-dBm to −130-dBm range, except for two points: (1) −105 dBm with DSS 12 pointing toward DSS 14 at the former's lowest elevation possible (32 deg for that hour angle/declination), and (2) −115 dBm with DSS 12 pointing at zero elevation angle near the southeastern horizon (azimuth = 150 deg). Although the 15.9-km separation should result in 4 dB more path loss than for the DSS 14/16 test, similar power levels were received. In any case, it appears that the power entering the DSS 12 receiving system is fairly independent of antenna pointing, as though the entire spillover for that antenna saw an enclosing "RFI blackbody" at a fairly uniform power level.

C. Test 3 (DSS 12, S-Band, Total Power, March 31, 1989)

A more comprehensive set of tests was made at DSS 12 approximately one month after Test 2. This time both test-signal comparison and AGC voltage were used to measure the 2320-MHz received radar signal. Figure 4 shows a polar plot of the AGC level (in dB) relative to the zenith power level of −127 dBm. The data taken cover virtually the entire sky from horizon to zenith, excluding the unreachable northern horizon. Except for the +22 dB point (−105 dBm), all data points lie in the range of −113 to −135 dBm. The highest point on this curve (+22 dB) is, as seen in Fig. 3, when DSS 12 points toward DSS 14 at about a 35-deg elevation angle. Other high points are at the horizon near azimuth 210 deg (14 dB above the zenith level) and low in the sky near azimuth 105 deg (+11 dB).

D. Test 5 (DSS 16, S-Band, Total Power, May 17, 1989)

During this test, azimuth restrictions on the DSS 14 transmitting antenna would not allow complete DSS 16 sky coverage for one consistent experiment condition. During the first two hours of the test, DSS 14 pointed at an azimuth of 195.1 deg, which was as far east as possible to the DSS 14/16 azimuth line of 171.2 deg. During the second two hours of the test, DSS 14 pointed toward DSS 16 at an azimuth of 171.2 deg. Throughout the test, DSS 14 transmitted 400 kW at an elevation of 15 deg. RFI was measured relative to a calibrated test signal as described above. Toward the middle of the test, an FET amplifier was installed, which allowed measurement of signals as low as −145 dBm. The only common set of data for the two DSS 14 azimuths was the DSS 16 scan at $Y = -30$ deg (westward). It was found that on the average the received power level *dropped* 6 dB when DSS 14 was pointed directly *toward* DSS 16, as opposed to the first half of the data taken when DSS 14 was pointed 24 deg westward (azimuth = 195.1 deg). This RFI decrease may be due to increased "line-of-sight" hill blockage, whereas the higher levels with nondirect pointing may be due to some multipath or diffraction effect.

Figure 5 shows the X-Y antenna coordinate system with received power levels indicated. All data shown without parentheses correspond to the line-of-sight (azimuth = 171.2 deg) condition. The $Y = 0$ points are the original data points (shown in parentheses, taken during the first two hours) decreased by the 6-dB loss determined above.

For the direct-pointing case (DSS 14 azimuth = 171.2 deg, toward DSS 16), received RFI power ranged from about −125 to −140 dBm, except for some hot spots near the northern horizon below 10-deg elevation, and a particular hot spot at an elevation of 26 deg and azimuth of 327 deg (see Fig. 5). For the nondirect pointing case (DSS 14 azimuth = 195.1 deg), this RFI range would be −119 to −134 dBm (6 dB higher), with correspondingly higher hot spots.

III. Radar Spectrum Tests

A. Theoretical Background

The purpose of these tests was to determine if there exists sufficient filtering or bandwidth limiting in the uplink exciter chain or the klystron amplifier to cause the modulated radar-spectrum amplitude at the top of the DSN bands to fall below the −192-dBm CCIR (International Radio Consultative Committee) limitation. Al-

though the modulated spectrum falls off in amplitude away from the carrier frequency, this alone is not sufficient to bring the RFI level down to −192 dBm at 2300 MHz.

Figure 6 shows the theoretical spectrum of a modulated S-band radar signal. The curve shown represents the envelope of nearly three hundred lines between 2295 MHz and 2320 MHz (the carrier frequency). The modulation used for this representation is that which would give the highest sideband power level for realistic radar signals transmitted by the DSN antennas (PN code length $p = 31$, digit period $t = 0.375$ μsec). It is seen that relative to the power at the carrier frequency of 2320 MHz, the power at 2300 MHz is down only 28 dB. It can be shown [1] that for any particular total power transmitted, the power of the peak line level of the modulated envelope is 15 dB below the total power level. The powers in all the individual lines add p to the total transmitted power. Thus by measuring the total RFI received power (CW, unmodulated) at the carrier frequency, one can equate that level to the power in all the lines of the *modulated* spectrum. As an example, if the total CW RFI power received is −120 dBm, the power in all the lines together of a *modulated* spectrum is −120 dBm. Since the envelope peak is 15 dB below the total, the modulated-spectrum absolute power level can thus be determined. In Fig. 6, for a total power of −120 dBm, the power level *per line* at 2320 MHz is thus −135 dBm, and the power *per line* at 2300 MHz is 28 dB below that, or −163 dBm. This power is 29 dB *above* the CCIR limit of −192 dBm. Obviously, additional filtering is required.

Figure 7 shows the theoretical spectrum of an X-band radar signal modulated identically to the S-band signal described above ($p = 31$, $t = 0.375$ μsec).

In the above examples, the assumed total received RFI power is −120 dBm. This represents an average upper limit of the S-band measurements described above. Of course, several hot spots were detected, but the antenna orientations for those measurements are not considered representative of normal DSN spacecraft tracking/radar pointing configurations.

X-band RFI measurements could not be made due to equipment limitations. Theory would indicate, however, that for the same transmitted powers, X-band RFI would be less than that at S-band, due to lower terrain diffraction (hence multipath) effects at that shorter wavelength. To first order, there appear to be no obvious antenna-related RFI differences such as spillover or quadripod diffraction. In the analyses that follow, it is assumed that X-band received RFI total power is −120 dBm (as in the S-band case), which may represent a worst-case scenario.

B. Test 4 [DSS 14, Radar Spectrum at Exciter-Chain Output (Klystron Input), S- and X-Bands, April 9, 1989]

Figure 8 shows the transmitter exciter-chain output spectrum measured at the klystron-amplifier input for code length $p = 31$, code period $t = 0.375$ μsec. Normalizing the spectrum to −120 dBm total received power (−135-dBm envelope peak) shows that at 2300 MHz the single peak has a power level of about −188 dBm.

The normalization to −120 dBm is somewhat arbitrary, but represents an average upper limit to the RFI received total power during the DSS 12 and DSS 16 tests, as described above. Obviously several hot spots existed during those tests, but the average RFI environment that existed was typically in the −120-dBm to −130-dBm range. At −130 dBm, the 2300-MHz signal shown here would have an absolute level of −198 dBm, 6 dB *below* the CCIR limit. Also shown is the theoretical modulated spectrum envelope for $p = 31$, $t = 0.375$ μsec. It is seen that at 2300 MHz, 25 dB of additional filtering has actually occurred, compared to the 29 dB needed.

Similar tests were made at X-band, and the modulated spectrum is shown in Fig. 9 along with the theoretical spectrum for the same code length and period. It is seen that significantly more filtering exists and the normalized power level at 8440 MHz (for −120 dBm total RFI power) is below −200 dBm, substantially below the CCIR −192-dBm limit.

C. Test 6 (DSS 14, Radar Spectrum at Klystron Output, S- and X-Bands, May 22, 1989)

Although the S- and X-band klystron input spectra described above indicate that for the RFI power levels measured at DSS 12 and DSS 16 sufficient filtering exists to meet CCIR RFI limits, additional tests were carried out to determine if undesired harmonics in the klystron existed or if additional klystron filtering would reduce the RFI problem.

Figure 10 shows the S-band 395-kW klystron output with $p = 31$ and $t = 0.375$ μsec. Comparison with the klystron input in Fig. 8 shows that no harmonics can be seen and that the output has slightly lower sidebands. Thus, it is evident that the klystron has an additional bandwidth-limiting effect. At 2300 MHz, the normalized power level (for −120 dBm total power) is about −202 dBm, a decrease of power deduced from the input spectrum of 14 dB (the input level being −188 dBm). Thus, for this case, even for RFI received-power levels

of −110 dBm (higher than virtually all the experimental field-test data, except the rare hot spots), the CCIR RFI limit of −192 dBm is met at 2300 MHz. At frequencies below this, the received power would decrease even more because of the steep rolloff of the measured modulated spectrum.

Figure 11 shows the X-band klystron *input* spectrum (measured on May 22, 1989, $p = 31$, $t = 0.375$ μsec) that is significantly different than that shown in Fig. 9. The difference in the two tests is that the synthesizers in the exciters differed, the first one producing more noise than the second. The klystron *output* spectrum taken the same day as the Fig. 11 *input*, using the same exciter input, is shown in Fig. 12. Comparison of Figs. 11 and 12 indicate virtually identical spectra, both with steeper rolloff than the earlier Fig. 9 spectrum. There appears to be no additional X-band klystron bandwidth-limiting effect, and it is assumed that an output spectrum corresponding to the Fig. 9 input will also be identical. In any case, since the Fig. 9 spectrum appears to satisfy the CCIR RFI limit by a substantial margin, use of the narrower-band modulation spectrum of the Fig. 12 case can only improve matters.

IV. Summary and Conclusions

A. Total Power Measurements

Figure 13 shows a chronological presentation of all 102 S-band RFI data points measured in the four field tests described in Section II. The 44 data points shown as "+" are for receiving-antenna elevations of less than 10 deg. Virtually all of the hot-spot points are at those low elevation angles. In particular, the high measurements above −100 dBm in the first 21 points were made at 4.5-deg elevation in a localized hot-spot direction (see Fig. 2). Only four data points with powers greater than −120 dBm are for elevations of 10 deg and higher. These four points represent only two distinct pointing conditions of the receiving antennas. Points 28 and 40 were obtained in Tests 2 and 3, respectively. The antenna pointing angles were practically the same for these two points. Points 66 and 67 were taken with identical pointing of the DSS 16 antenna during Test 5 (see Fig. 5). Thus, there are only two high-elevation RFI hot spots in this data set. The antenna pointing angles for the four points described above are shown in Table 1.

Seventy-five points have powers of −120 dBm or lower. Disregarding the points below 10 deg, there are only two points each for DSS 12 and DSS 16 that are above −120 dBm; fifty-four points are −120 dBm or lower. This supports the use of −120 dBm in the theoretical modeling described in Section III. Other than the general −120-dBm upper limit for each site, it is difficult to characterize one or the other of the sites as having a "better" RFI environment.

The low-elevation hot-spot RFI may be a result of metallic objects reflecting hill-diffracted radar signals into the face of the receiving antennas. Because the lower edge of all the antennas is very near the ground at low elevation angles (5–20 ft in most cases), nearby objects such as microwave relay towers and their 6–8-ft diameter dishes, floodlight posts, air-conditioning ducts and blowers, collimation towers, and water tanks may all be within the near-field cylindrical beam of the receiving antenna. Multipath from hill, to metallic reflector, to quadripod, to feedhorn may be a cause of RFI. Additionally, significant "isotropic" RFI may be due to sidelobe and backlobe response to radar signals reflected from the myriad metallic objects located within miles of each antenna. In other words, although the antenna might be pointed at a high elevation angle, the backlobes are receiving RFI from objects on the ground, behind the antenna. It is suggested that future investigations of these effects be made and tests carried out to develop methods of reducing this problem.

X-band RFI measurements could not be made, but it is believed (as stated in Section III.A) that X-band received powers would be somewhat less than the corresponding S-band powers for the same antenna-pointing configurations because of decreased diffraction/multipath effects at the higher frequency.

B. Exciter-Chain Output and Klystron Output Spectrum Tests

Measurements of exciter-chain output spectrum and klystron output spectrum at both S- and X-bands indicate significant bandwidth filtering beyond the mathematical rolloff of modulated radar signals. Using a theoretical model of a worst-case spectrum ($p = 31$, $t = 0.375$ μsec) and a total received power of −120 dBm, it is shown that the additional filtering presently existing in the radar uplink at DSS 14 (in excess of 20 to 30 dB) appears sufficient to reduce the received power levels at the top of the DSN receiving bands (2300 MHz and 8440 MHz) to below the CCIR limit of −192 dBm for a 1-Hz bandwidth. However, if the radar bandwidth is increased in the future, this limit may be exceeded.

Acknowledgments

The authors wish to thank the following people for their assistance in carrying out the Goldstone RFI study reported here: John Sosnowski, Erik Holmgren, Chuck Goodson, Dennis Choate, and Larry Sturgis helped us in making the RFI measurements; Reg Cormier carried out the transmitter spectrum tests; Al Banji and Ray Jurgens advised us on numerous radar matters; and Mike Brown and Dee Yeaman arranged operations support and scheduling for all these tests.

Reference

[1] W. C. Lindsey and M. K. Simon, *Telecommunication Systems Engineering*, Englewood Cliffs, New Jersey: Prentice-Hall, 1973.

Table 1. Antenna-pointing parameters for four points with powers greater than −120 dBm

Point	Station	Azimuth, deg	Elevation, deg	RFI Power, dBm
28	DSS 12	333	32	−105
40	DSS 12	331	35	−105
66	DSS 16	326	26	−115
67	DSS 16	326	26	−112

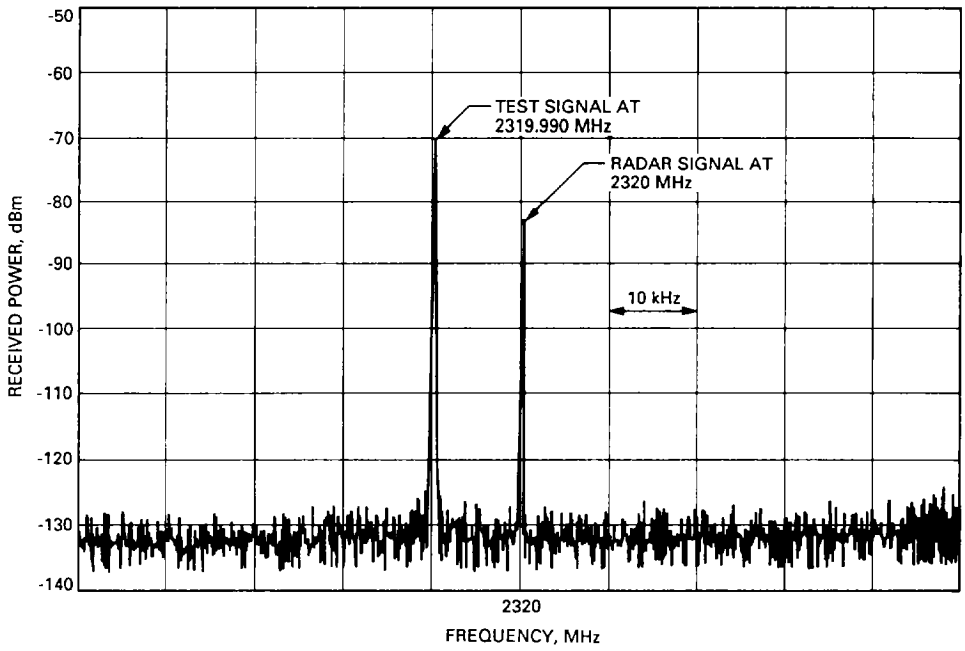

Fig. 1. Test 1: DSS 16, January 27, 1989, −70-dBm test signal and −83-dBm radar RFI at 2320 MHz.

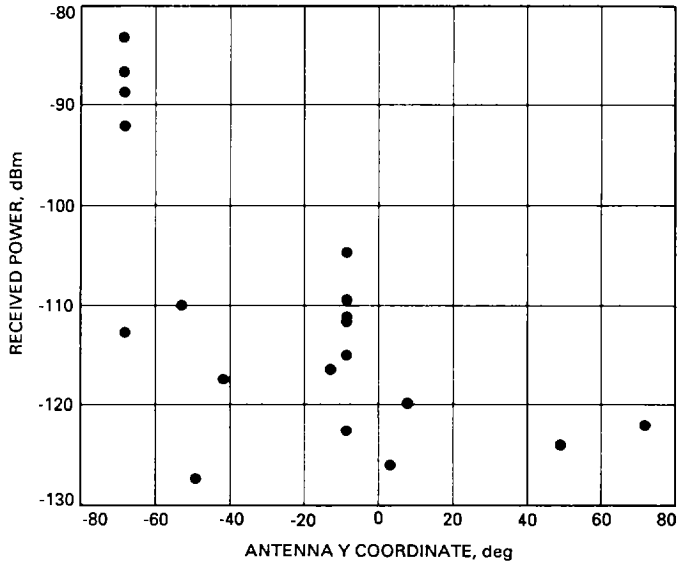

Fig. 2. Test 1: DSS 16, January 27, 1989, radar RFI versus DSS-16 pointing, elevation = 4.5 deg.

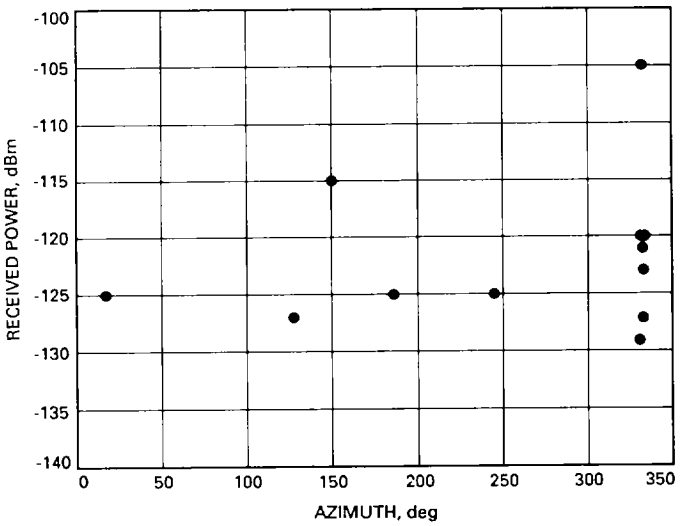

Fig. 3. Test 2: DSS 12, February 27, 1989, radar RFI versus DSS-12 pointing.

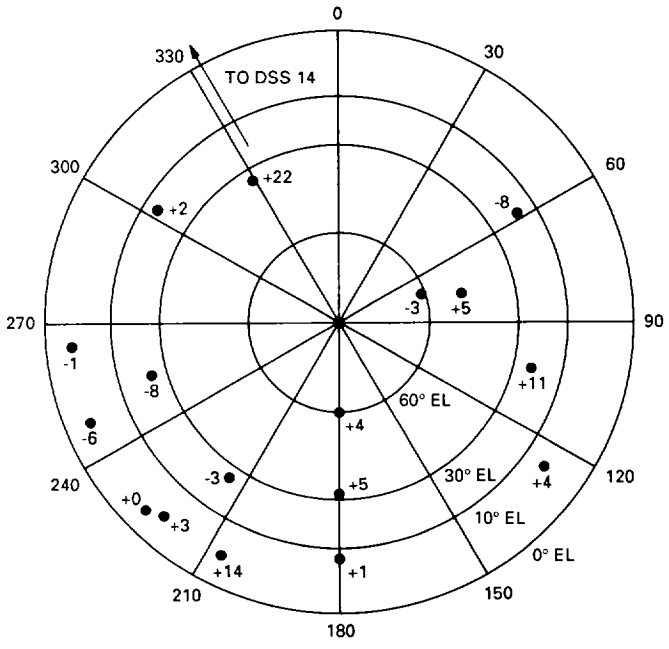

Fig. 4. Test 3: DSS 12, March 31, 1989, radar RFI versus DSS-12 azimuth-elevation pointing, referenced to zenith power level of −127 dBm.

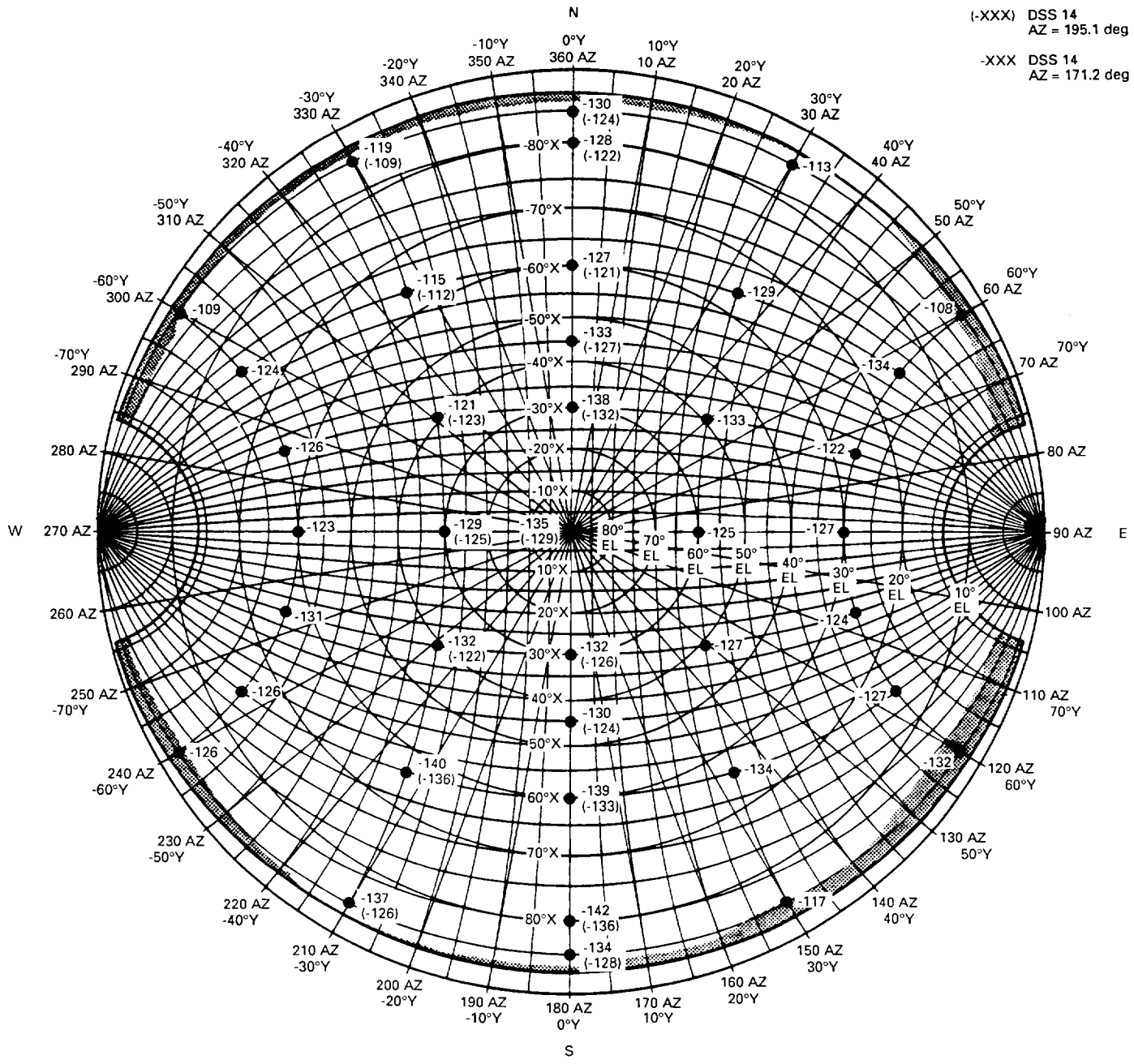

Fig. 5. Test 5: DSS 16, May 17, 1989, radar RFI versus DSS-16 X-Y pointing, DSS-14 power = 400 kW at 15-deg elevation for all points.

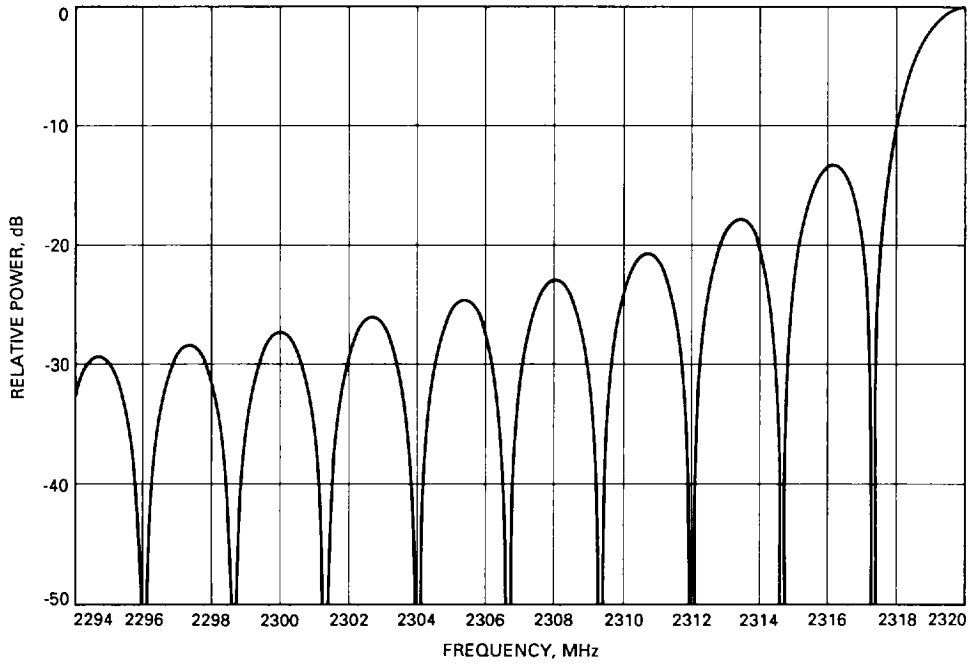

Fig. 6. Theoretical modulated S-band radar spectrum for $p = 31$, $t = 0.375$ μsec.

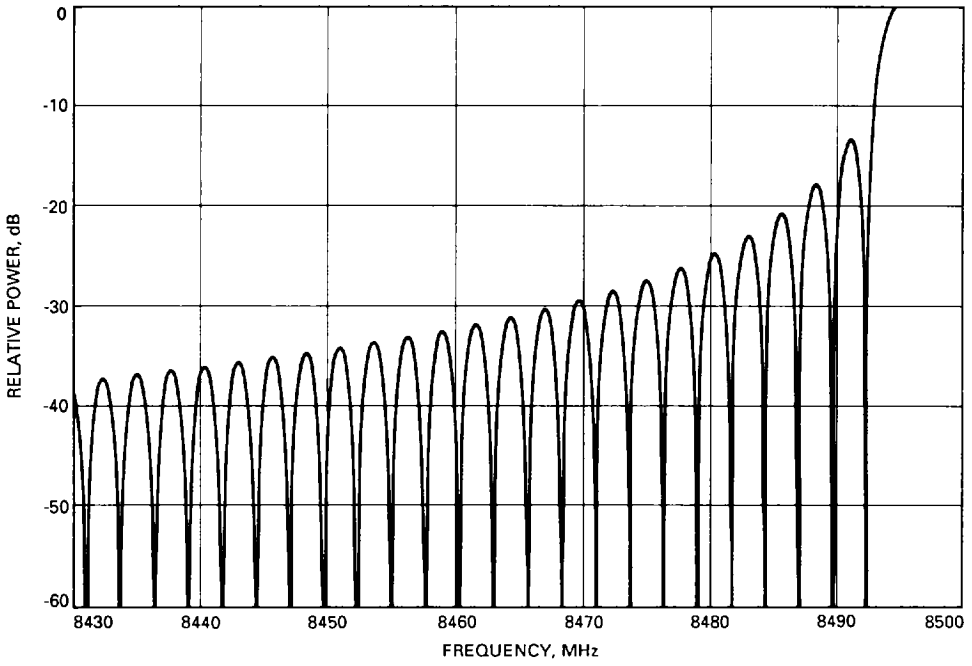

Fig. 7. Theoretical modulated X-band radar spectrum for $p = 31$, $t = 0.375$ μsec.

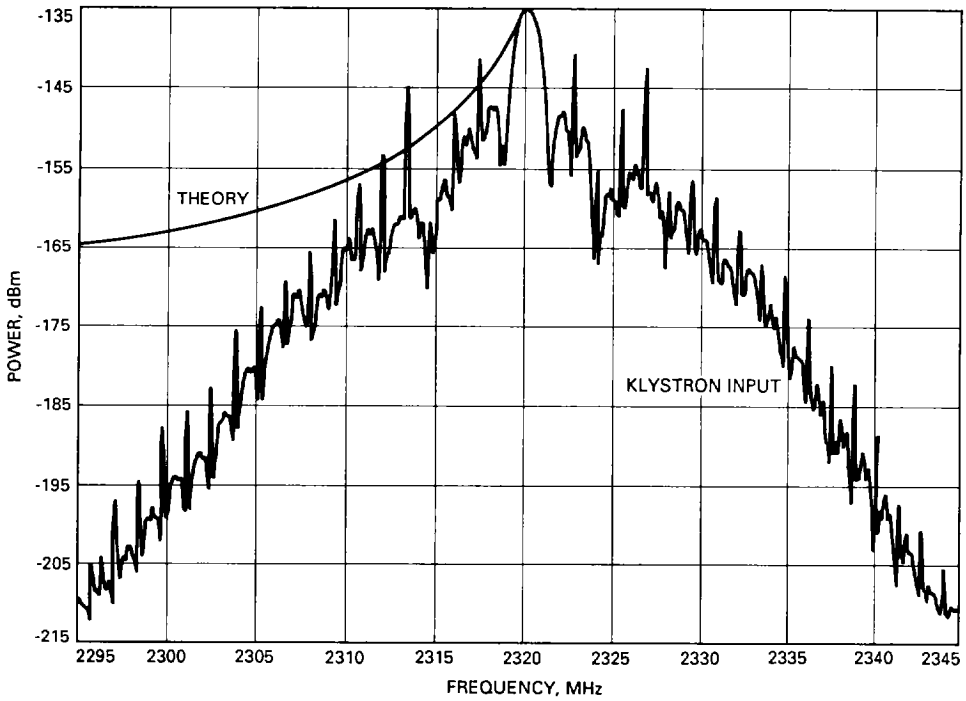

Fig. 8. Test 4: April 9, 1989, S-band exciter-chain output (klystron input) spectrum and theoretical modulated spectrum for $p = 31$, $t = 0.375$ μsec.

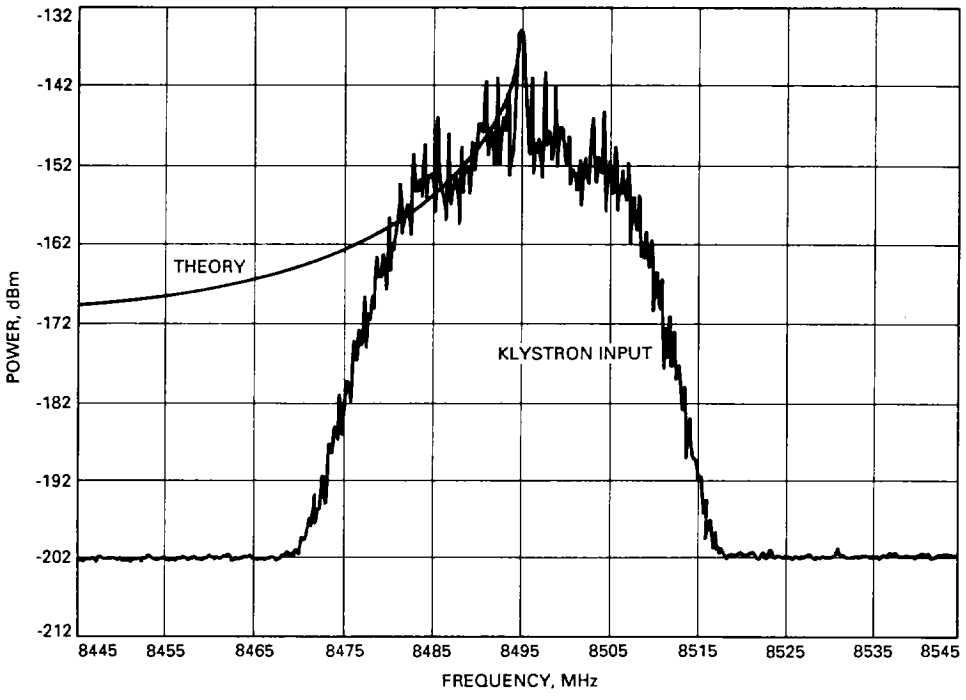

Fig. 9. Test 4: April 9, 1989, X-band exciter-chain output (klystron input) spectrum and theoretical modulated spectrum for $p = 31$, $t = 0.375$ μsec.

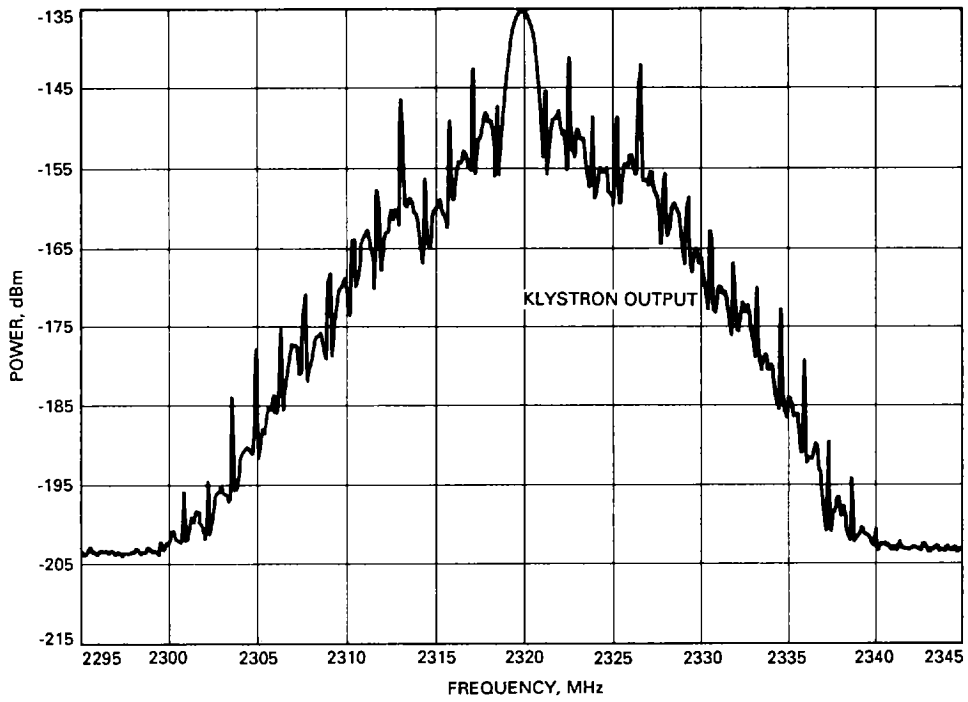

Fig. 10. Test 6: May 22, 1989, S-band klystron output spectrum, $p = 31$, $t = 0.375$ μsec.

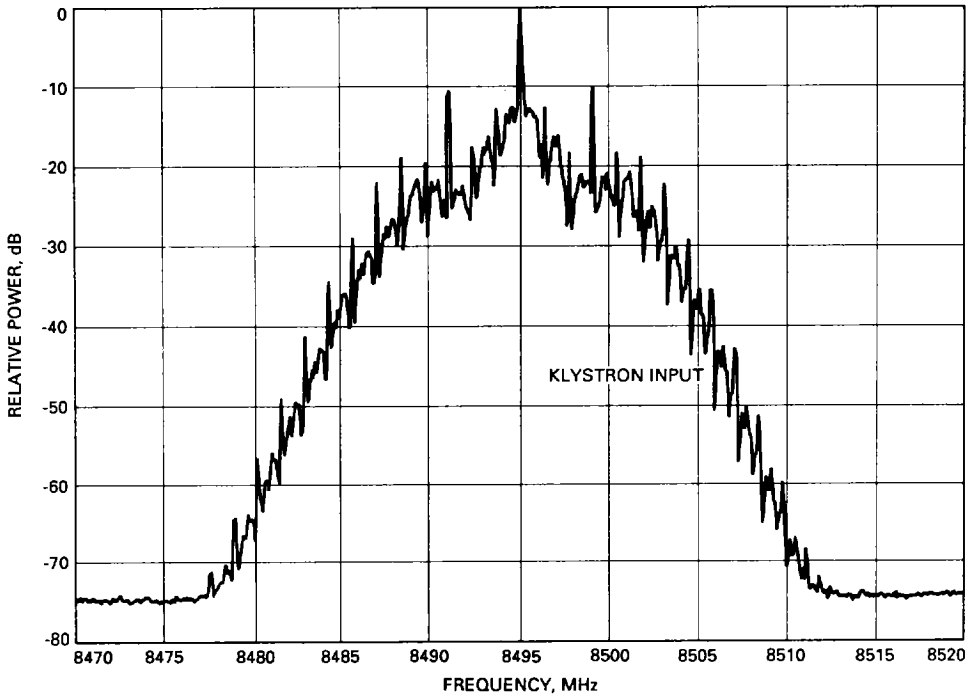

Fig. 11. Test 6: May 22, 1989, X-band klystron input spectrum, $p = 31$, $t = 0.375$ μsec (compare with Fig. 10).

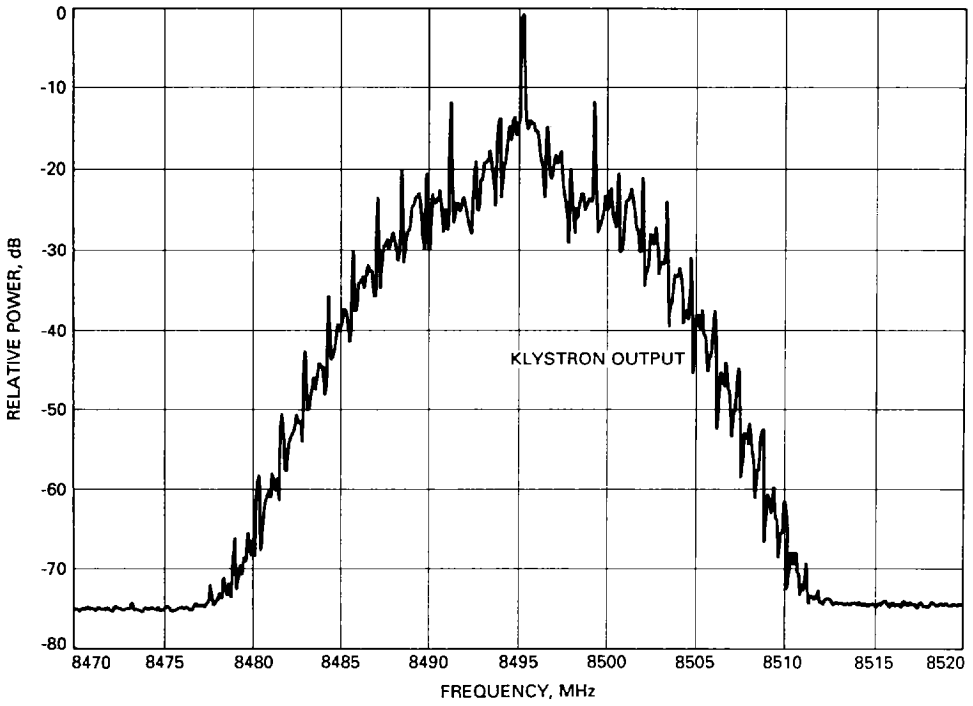

Fig. 12. Test 6: May 22, 1989, X-band klystron output spectrum, $p = 31$, $t = 0.375$ μsec.

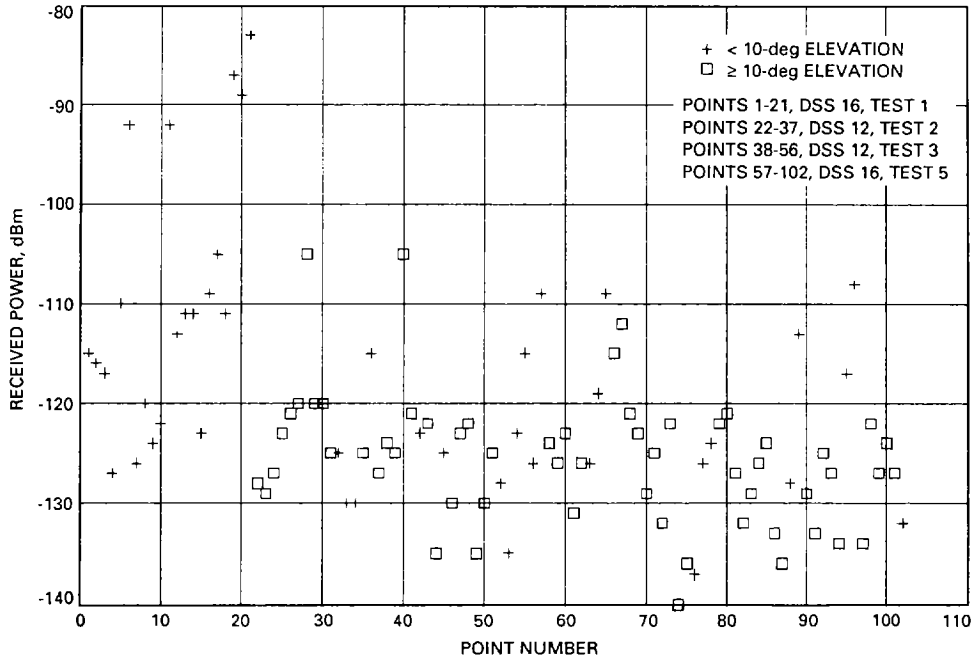

Fig. 13. S-band radar RFI data, all tests.